International Journal on Science and Technology (IJSAT)
E-ISSN: 2229-7677 ● Website: www.ijsat.org ● Email: editor@ijsat.org

Experimental Evidence of Capillary-Dominated Entirely Detached Growth in a Vertical Directional Solidification (VDS) Process Under 1g

Dattatray Gadkari

Independent Researcher, Shree Yogesh Tower, Kora Kendra, Borivali (W), Mumbai, India

ABSTRACT

Entirely detached crystal growth under terrestrial gravity has been experimentally observed in the VDS process since the 1994s, yet its physical origin has remained unresolved within classical solidification theory. Conventional gravity-based criteria implicitly assume continuous mechanical contact between the melt and the container wall, leading to buoyancy-driven convection and gravity-influenced interface instability. In contrast, VDS experiments consistently demonstrate sustained wall-decoupled growth, characterized by a stable gas-filled gap between the crystal and the container and by microgravity-like transport behaviour under 1g conditions.

Stability maps constructed in Bond number–Capillary number space show that VDS experimental conditions lie deep within the capillary-dominated regime, whereas conventional growth systems remain gravity-controlled. Dewetted Bridgman and microgravity solidification data occupy intermediate and overlapping regions, providing independent validation of the proposed framework. These results demonstrate that sustained detached growth under terrestrial gravity arises from capillary stabilization rather than gravity reduction, establishing VDS as a practical terrestrial analogue of microgravity solidification.

In this work, we present a combined experimental and dimensionless analysis that establishes entirely detached growth in VDS as a *capillary-dominated solidification regime*. Systematic growth experiments on Sb-based semiconductor systems reveal stable detached interfaces, suppressed transverse transport, improved crystallographic quality, and reduced defect densities compared with conventional wall-contact growth. By explicitly incorporating capillary effects through the Bond and Capillary numbers, we formulate the *Gadkari Detached Stability Criterion (GDSC),* which quantitatively distinguishes gravity-influenced wall-contact growth from capillary-dominated wall-decoupled growth.

Keywords: VDS detached process; Sb-based solidification; Capillary-driven growth; Young–Laplace Effect; Mullins–Sekerka stability; Soret effect; Gadkari Stability Criterion; Microgravity analog;

1. Introduction

Solidification is a fundamental route for producing bulk crystalline materials and semiconductor ingots. Under terrestrial conditions, however, solidification is inevitably influenced by gravity through hydrostatic pressure, buoyancy-driven convection, and container–melt interactions. In conventional crystal growth techniques such as Bridgman and Vertical Gradient Freeze (VGF), the growing crystal remains in continuous contact with the container wall. This contact introduces mechanical constraint, thermal stress, and interfacial shear, while gravity-driven melt flow perturbs solute and temperature fields near the crystal–melt interface, often resulting in interface instability, radial segregation, and high defect densities (Incropera et.al.2000; Lan et.al 2002, Derby et.al. 2012).

Capillary effects have long been recognized as an essential stabilizing influence at fluid–solid interfaces. Surface tension governs interface curvature and pressure balance through the Young–Laplace relation and plays a decisive role in interface morphology at small length scales (Bonn et.al 2003; Rowlinson et.al 2006). In most terrestrial solidification systems, however, capillary forces are masked by gravity and viscous effects, restricting their influence to local interface smoothing rather than global growth stability. As a result, classical solidification theory has largely evolved within a gravity-dominated framework emphasizing buoyancy-driven transport and convection–diffusion coupling (Kurz et.al.2002; Duffar et.al. 2000); Wang, et.al 2004).

Detached or dewetted solidification represents a fundamentally different growth mode. In this configuration, the crystal solidifies without mechanical contact with the container wall, sustained by a capillary-supported gap between the solid and the crucible. Post-2000 experimental studies demonstrated that such detached growth can significantly reduce wall-induced stresses, suppress transverse transport, and improve crystal quality (Bizet et.al. 2004; Gadkari et.al. 1997; 2004). Nevertheless, under terrestrial gravity, detached growth was generally considered difficult to sustain because gravity-induced hydrostatic pressure and melt convection tend to destabilize the meniscus and promote reattachment (Gadkari et.al. 2009; Chevalier et.al. 2004; Palosz et.al. 2005).

Microgravity experiments provided crucial insight into this problem. Directional solidification studies performed under reduced gravity consistently revealed diffusion-dominated transport, stable interfaces, and markedly improved compositional and structural uniformity compared with Earth-based growth (Balint et.al (2008); Akamatsu et.al. 2023; Bergeon 2021). These experiments clearly demonstrated that suppression of gravity-driven convection stabilizes the crystal–melt interface and reduces defect formation. However, routine access to microgravity platforms remains limited, motivating the search for terrestrial growth methods capable of reproducing similar physical conditions.

Within this context, the VDS process emerged as an unconventional but reproducible approach to crystal growth under terrestrial gravity. In our earlier investigations, we demonstrated that VDS-grown Sb-based semiconductor crystals exhibit a continuous and stable gap between the crystal and the ampoule wall, resulting in *entirely detached growth under 1g conditions (Gadkari 2012-2020; 2025)*. Optical inspection, post-growth sectioning, and crystallographic characterization confirmed that this gap persists over extended growth lengths, indicating complete mechanical decoupling of the crystal from the container.

A defining feature of detached growth in VDS is the systematic evolution of the crystal–melt interface from concave to planar and finally to a convex morphology during growth, without reattachment to the wall (Gadkari et.al. 2009; Epure et.al. 2010; Stelian et.al. 2009). This behavior is accompanied by reduced dislocation density, improved orientation uniformity, and suppressed radial compositional variation compared with conventional container-contact growth. Such observations cannot be reconciled with classical gravity-dominated solidification descriptions, which predict strong buoyancy-driven convection and interface distortion under comparable thermal gradients.

Independent studies on dewetted Bridgman growth have shown that the stability of detached states is governed by the balance between hydrostatic pressure and surface-tension-driven capillary pressure at the meniscus (Mazuruk et.al. 2013; Balint et.al. 2012; Yu et.al. 2019). Analytical and numerical analyses based on the Young–Laplace relation demonstrate that when capillary pressure exceeds gravity-induced pressure, stable detachment can be sustained even under terrestrial gravity (Schwabe et.al.2002; Shevtsova et.al. 2003; Kakimoto et.al. 2005). These findings indicate that detached growth is not inherently restricted to microgravity but can occur whenever capillarity dominates the force balance at the interface.

The VDS configuration naturally promotes this capillary-dominated regime. Unlike Bridgman and VGF systems, where wall contact enforces no-slip boundary conditions and enhances buoyancy-driven convection (Tourret et.al. 2015; Volz et.al. 2011) VDS eliminates direct mechanical coupling between the melt and the container. As a result, transverse transport is strongly suppressed and solute redistribution becomes predominantly axial, leading to quasi-one-dimensional, diffusion-controlled solidification (Medjkoun et.al. 2025).

Comparisons with microgravity directional solidification further support this interpretation. Microgravity experiments report planar or weakly curved interfaces, low segregation, and reduced defect densities—features that closely resemble those observed in VDS detached growth under terrestrial gravity (Gadkari et.al. 2012; 2013; 2025). Transport anisotropy metrics reported in VDS experiments fall within the same range as those measured in microgravity studies, reinforcing the physical equivalence of the two growth environments (Gadkari et.al 20013-16).

The present work builds upon our previous experimental studies (Gadkati 1997; 2004; 2009; 2012-2020; 2025) and provides a unified experimental and physical interpretation of entirely detached growth in the VDS process. By combining systematic growth experiments with dimensionless analysis, we demonstrate that VDS operates in a *capillary-dominated solidification regime*, where surface-tension forces overwhelm gravity-driven instabilities. This framework resolves the long-standing question of entirely detached growth stability since 1994s under 1g conditions and establishes VDS as a terrestrial pathway toward microgravity-equivalent crystal growth.

Experimental Procedure

Vertical Directional Solidification (VDS) Configuration

Crystal growth experiments were performed using a vertical furnace designed as shown in Fig-1 to promote axial heat flow and minimize transverse thermal gradients. The growth assembly consists of a vertically oriented quartz tube (diameter 10cm, length 100cm) as growth chamber for housing a sealed

quartz ampoule. The ampoule geometry comprises a cylindrical body with a conical bottom section and a hemispherical top, ensuring uniform wall thickness and mechanical symmetry along the growth axis.

The ampoule was evacuated and sealed prior to growth, establishing a controlled internal pressure environment. This configuration enables the formation of a stable gas-filled gap between the growing crystal and the ampoule wall during
solidification. Unlike conventional Bridgman or VGF systems, no intentional contact between the crystal and container wall is enforced during growth.

Crystal growth experiments were performed in a custom-built vertical furnace providing an increasing axial temperature gradient. The growth chamber consisted of a vertical quartz tube and a sealed quartz ampoule. The ampoule had a cylindrical body (inner diameter 10–22 mm, wall thickness 1.5–2 mm), a conical bottom section (cone angle ≈ 45-65°), and a hemispherical top.

Prior to sealing, the ampoule was evacuated to a pressure below 10^{-5} mbar and flame sealed. After sealing, the residual internal pressure at growth temperature was estimated to be in the range ~200 Pa, depending on temperature and vapor pressure of the melt. This low internal pressure is essential for enabling capillary-supported detachment between the crystal and the ampoule wall. No vibration, or magnetic field was applied during growth. Some growth cases an ampoule rotation (10rpm) was used, however no as such effect on crystal quality, since growth is independent of rotation, and depended on translation rate.

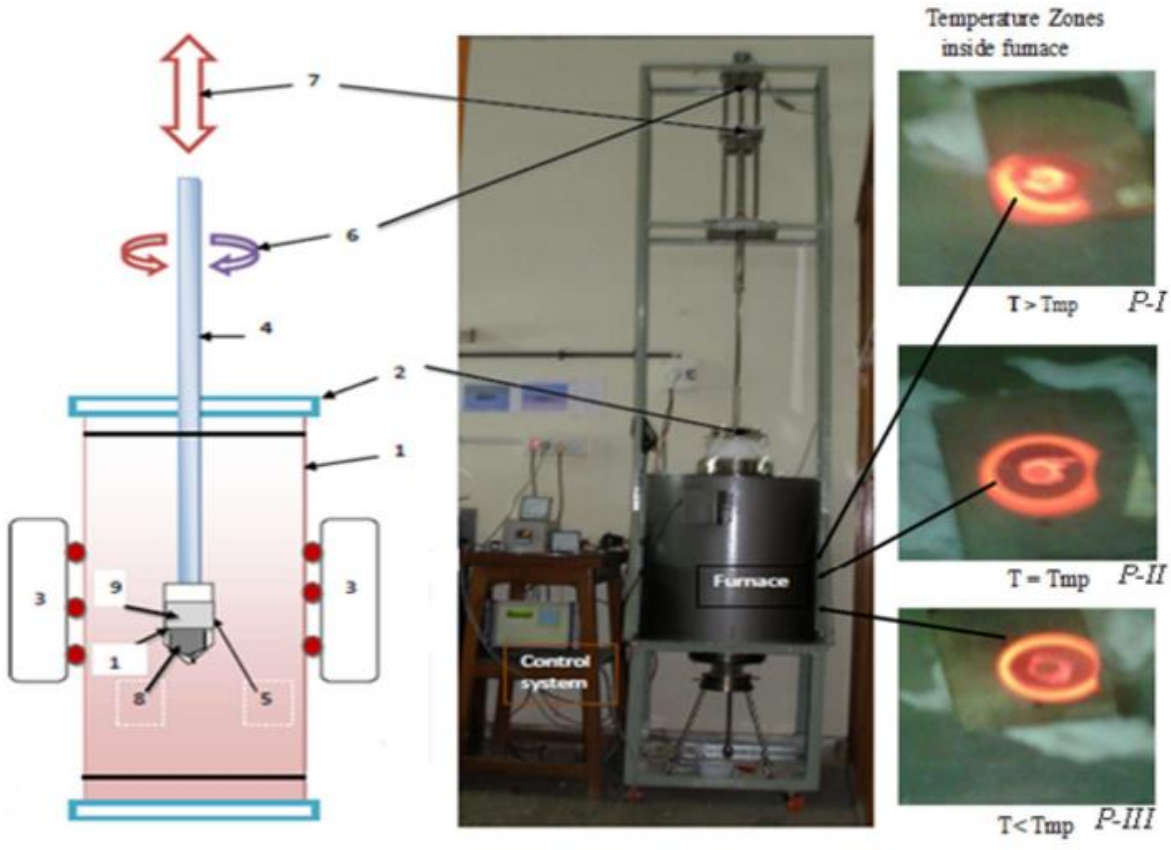

(a) (b) (c)

Fig.1 (a**) s**chematic of the VDS process numbers represent: 1. Melt, 2. Wilson seal, 3. The vertical furnace profile, 4. Shaft, 5. Quartz ampoule, 6. Clock-anticlock rotation, 7. Up-down, 8. Detached crystal, 9. Vacuum, 10. quartz tube, (b) the photo of true VDS process, and (c) the thermal images inside vertical furnace at three regions PI is the centre 850^0C at 33cm, PII is middle temperature 700^0C at 17cm, and PIII is lower temperature 525^0C at 13cm height from bottom of furnace.

Materials and Charge Preparation

High-purity elemental starting materials were used for all growth experiments: Indium (In): 5N purity, Gallium (Ga): 5N purity, and Antimony (Sb): 5N purity. Stoichiometric amounts corresponding to InSb, GaSb, and $In_{(1-X)}\,Ga_X\,Sb$ ($x \approx 0.1–0.5$) were weighed with an accuracy better than ±0.1 mg and loaded into the quartz ampoule inside an argon gas Table 2-3.

The sealed ampoule was placed in the furnace hot zone and held at temperatures at 850°C for 12 h to ensure complete melting of source materials and compositional homogenization Fig. 2, and some growths rotation was employed; homogenization occurred purely by diffusion and thermal convection within the melt.

Thermal Gradient and Growth Conditions

Directional solidification was achieved by translating the ampoule downward through increasing axial temperature gradient. The temperature profile consisted of a hot zone and a cold zone separated by a well-defined gradient region. Typical experimental parameters were: Growth hot zone temperature: 525–712°C (material dependent), Cold zone temperature: 350–500 °C, Axial temperature gradient at the interface: 8–20 $K \cdot cm^{-1}$, and Ampoule translation (growth) rate: 2–5$mm \cdot h^{-1}$

From previous growths, the growth rates (2. 5$mm.h^{-1}$) were deliberately kept low to suppress constitutional supercooling and to maintain a stable crystal–melt interface. Under these conditions, no cellular or dendritic breakdown of the interface was observed.

Importantly, transverse temperature gradients were estimated to be at least one order of magnitude smaller than the axial gradient, ensuring quasi-one-dimensional heat flow.

Table 1 Thermal and process parameters used in VDS Growth process (Core experimental conditions defining seed formation, detachment, and entirely directional solidification)

Sr. No.	Parameters	Values / Range	Physical role in VDS	Notes
1	Furnace type	Vertical, Single zone	Provides axial heat flow	Low radial symmetry ($<0.5^0$C)
2	Axial gradient (G)	10-32^0C	Control interface stability	Matches gradient used in ISS or controlling equipment
3	Growth rate (V)	2 to 5mm/h	Ensure diffusion-dominated growth	Lower V suppresses cellular instability
4	Thermal condition (T)	525-715^0C	Onset crystallization – self-oriented seed	Supercooling < 5^0C

5	Melt super heat	10-15^{0}C	Ensures full melt homogenization	Avoids premature nucleation
6	Vacuum gap thickness	70-250µm	Decouples melt from wall	Capillary pressure > hydrostatic
7	Melt column height	40-75mm	Determines hydrostatic load	Young-Laplace requirement satisfied
8	Meniscus curvature radii (R1, R2)	0.7-1.6mm	Set capillary pressure	Stable curvature from bottom to top
9	Atmosphere	Ampoule, Sealed vacuum	Promotes melt-vapour interface	Essential for detachment

Experimental Evidence of Entirely Detached Growth

The charge contained vacuum sealed ampoule is hanged from shaft in Fig. 1 which was translated downward with a constant translation velocity (3mm/h), and rotation (10 rpm) throughout growth. Thermal field inside the furnace is shown in Fig. 1(c), where, the system's thermal field was controlled by PID controller. For heating the source materials into sealed ampoule, the temperature profile in Fig. 2 (a) was applied, then temperature raised to 850°C using this temperature profile to melt the source materials. However, the thermal conditioning was performed for 12h for congruent mixing of source materials for Sb-based materials Sb growth, but it varies according to the source materials. The seven steps growth profile cyclogram in Fig. 2(b) was applied for the detached growth, the growth details are in Fig. 2(b). In VDS process, the temperature gradient increases along crystal growth axis are added advantages for entire detached growth. The initial nucleation occurs at the conical bottom at lower temperature of grown ingot, but in entire detached growth freezing depends on the solidification point (melting point, and not on weight (weightlessness influence). This stage is critical, since, the self-oriented in-situ seed forms, which self creates the vacuum gap and entire detachment into VDS process, because the Young–Laplace capillary forces exceed hydrostatic pressure, and convection is minimized, the as grown ingots are shown in Fig. 3, the crystal-melt interface morphology on the surface of ingot is smooth and no any defects during growth, The interface morphology is consistently transfer from the beginning, this can be observed from the detached ingots surfaces. In fig. 3, entire detached ingots, (a) the GaSb: Mg as grown ingot into ampoule, (b) its free movement inside sealed ampoule, (c) the ternary detached ingots out of ampoule, (d) the InSb, and (e) GaSb detached ingots taken out of ampoule. The first grown region (tip) of all ingots reveals the concave shape, while last grown region of ingot attributed to the convex shape, showing the conversion of interface, Concave–Planar–Convex, these data and surface morphology of these ingot reveals successful entirely detached ingots growth VDS process. The identical interface shapes were observed in microgravity growth on ISS. Full-length detached VDS crystals, showing smooth surface, absence of wall adherence, stable meniscus signature, and complete crystallographic continuity from seed to top.

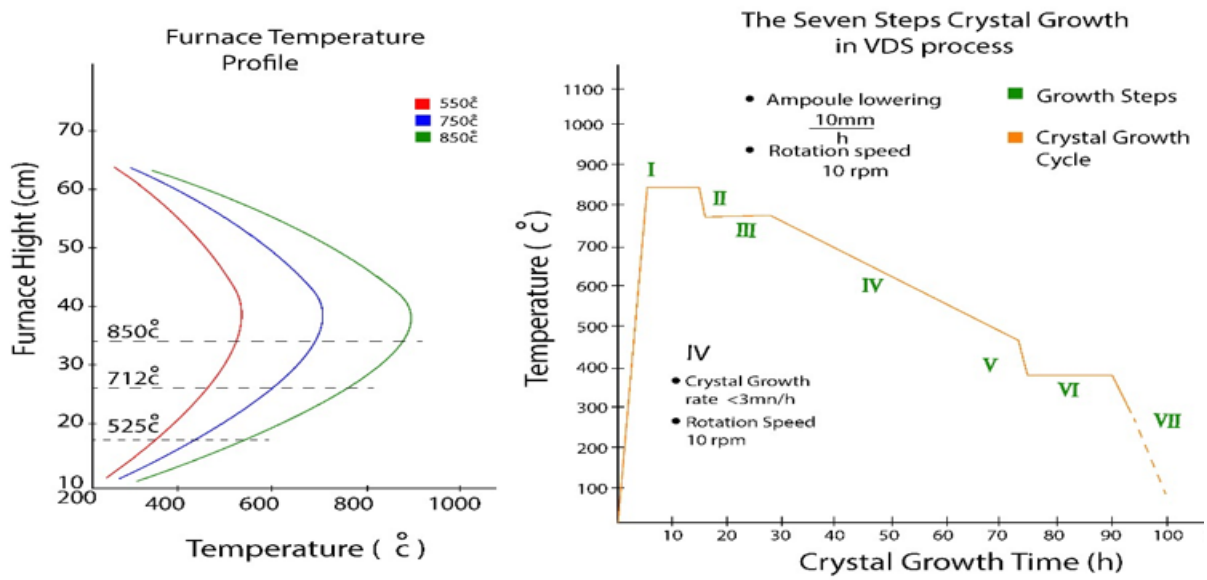

Fig. 2 (a) the thermal profile of vertical furnace, and (b) the typical seven steps detached VDS growth process

Entirely detached growth was confirmed through post-growth structural analysis. During growth, a continuous gap (70–250μm**)** between the crystal and the ampoule wall was developed over of crystal length (length 40mm-75mm) depending on growth conditions. After solidification, ingots came by a simple tapping an ampoule, the ingots were transvers and longitudinally sectioned (300μm). Optical microscopy confirmed the absence of crystal–wall contact over all the grown length (> 80 ingots), with a measured gap width (70–250μm) typically in the range Table 2-3. No localized contact was observed, some cases only near the initial seeding region. The crystal–melt interface showed a reproducible evolution from convex to planar and finally to convex morphology as growth progressed, while remaining fully detached from the container wall.

Structural and Crystallographic Characterization

The VDS process is designed to achieve entirely detached crystal growth under terrestrial gravity through a combination of controlled thermal fields, capillarity-driven melt support, and minimisation of interfacial free energy. The essential feature distinguishing VDS from conventional methods (Bridgman, VGF, and Czochralski) is the deliberate creation of a stable vacuum-gap configuration between the melt and the ampoule wall, allowing the melt column to be supported primarily by surface tension, not hydrostatic pressure. Therefore, the as grown detached ingots (Fig. 3, 4) were used for characterizations, here, these figures demonstrate the as grown entirely detached ingots growths. Multiple characterization techniques were employed: XRD (Cu-Kα): To determine seed orientation; EPD (etch-pit density): To quantify dislocation density; Electron microprobe/EDS: To examine radial and axial segregation; SEM: For interface morphology; Optical microscopy: For vacuum-gap verification, the growth deviation (GD) analysis: Using calibrated axial composition profiles. These experimental data serve as direct evidence of microgravity-equivalent conditions realized in the VDS system; the various materials characterizations are reported.

Crystal quality was assessed using X-ray diffraction (XRD) and chemical etching. XRD patterns showed dominant single-crystal reflections, primarily along (220) or (111) orientations, with no detectable secondary phases. The full width at half maximum (FWHM) of the rocking curves was typically < 128 arcsec Table 2-3.

Etch-pit density measurements revealed dislocation densities in the range 10^3–10^4 cm^{-2}, significantly lower than those typically reported for container-contact growth of comparable materials under terrestrial conditions. Axial compositional uniformity was confirmed by energy-dispersive X-ray spectroscopy (EDS), showing variations within at. %, while radial segregation remained below detection limit within experimental uncertainty Table 2-3.

(a) (b) (c) (d) (e)

Fig. 3 The comparison of typical entirely detached ingot in VDS process is given here, (a) as grown GaSb:Mg ingot, (b) the free movement of GaS:Mg ingot reveals the contactless growth, (c) the as grown $In_{0.5}Ga_{0.5}Sb$ ingot after washing, cleaning, and polishing, (d) The as grown InSb detached ingot, and (e) the as grown GaSb detached. For all entirely detached ingots into VDS process, first grown tip has concave interface, while last grown ingo has convex interface.

All ingots display the crystallographic appearance with a concave tip (seed), the last grown region displays the convex appearance of growth. XRD analysis confirms the presence of (220) diffraction peaks, which correspondence to (110) orientation growth of plane (crystallographic planes), demonstrating thermodynamically governed orientation selection. This self-generated seed provides a stable structural foundation for fully detached growth into VDS process. During VDS growth, a stable 70–250 μm vacuum gap forms between the as grown crystal and the ampoule wall. VDS process achieves outcomes equivalent to microgravity observations. Experimental data demonstrate that at the 1-g., the VDS crystals show: i) Growth deviation (GD) values between 0.015 and 0.028 [1,2], ii) fully detached lengths of 40–75 mm, iii) the planar to slightly concave interfaces, iv). uniform diffusion-controlled segregation, and v) dislocation densities of 0.62×10^3–$8.9\times10^3 cm^{-2}$ (equivalent to space-grown III–V crystals), and vi). fully detached

lengths of 40–75 mm, and measurements more details of ingots (> 80) in Table 2-3 for the several entirely detached growths in the VDS process.

Results

Experimental Evidence of Entirely Detached Growth

Figure 4, the process of taking out detached ingot from the ampoule, (a) the free movements of as grown ingot, (b) the sealed top of ampoule is cut to takeout as grown ingot, (c) The empty ampoule and visible marking of Sb coating inside ampoule wall as a grey colour of , (d) As grown ingot is outside, (e) Schematic enlarged view of the detached ingot growth showing top as the convex at last growth, and clear visibility of the Sb coating on the inner wall of an ampoule below the convex surface, while below is the tip (oriented in-situ grown seed), which has concave interface shape under capillarity force seen from top of ingot (d), and (f) Schematic principle of capillarity, the detached growth hypothesis is aligned with formation of self-oriented Seed and Young–Laplace meniscus in VDS. The meniscus curvature is capillary-supported melt surface (melt zone) and self-oriented seed. A Schematic of Fig. 4(f), the VDS standard ampoule geometry showing cylindrical body, conical bottom, and un-defined shape of a sealed top. In ternary growths, the InSb–$In_{0.5}Ga_{0.5}Sb$–GaSb triple-layer phase growth (charge) is arranged vertically by thermal conditions. Thin black inner separators indicate layer boundaries. The vacuum gap region, melt meniscus location, and expected capillary curvature are marked. This geometry forms the basis of detached growth. The black downward arrow is translation velocity of an ampoule and gravity force, where the detached growth is opposite the gravity vector.

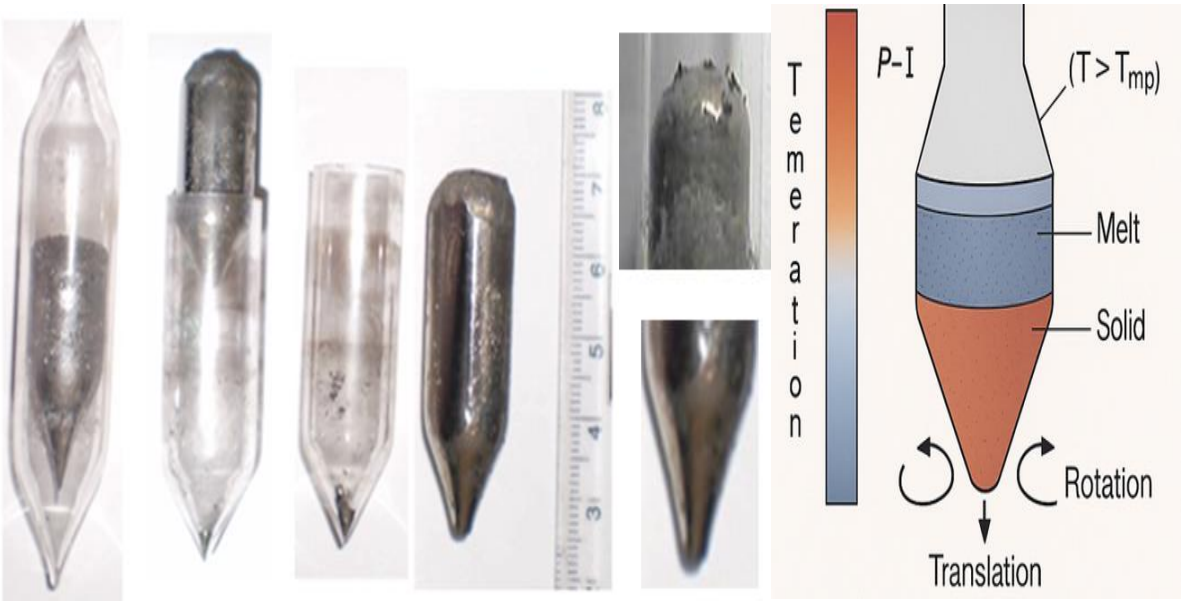

(a) **(b)** **(c)** **(d)** **(e)** **(f)**

Fig. 4, the typical process to take out detached ingot from vacuum sealed ampoule (a-e), and schematic ingot in (f)

These growth (Fig. 3, 4) shows the characteristic VDS growth configuration in which a continuous gap is maintained between the growing crystal and the ampoule wall. During growth, optical observation through the quartz ampoule revealed a stable detached gap extending of the crystal length. Post-growth longitudinal sectioning confirmed the absence of crystal–wall contact over all the grown region, with measured gap widths in the range of 70–250µm. Entirely detached growth was reproducible across

multiple growth runs and material systems Table 2-3, including InSb, GaSb, and $In_{(1-X)}Ga_XSb$. Localized contact was occasionally observed near the initial seeding region in conical section, whereas the remaining crystal was fully detached.

The evolution of the crystal–melt interface during VDS growth, at the initial stage of growth, the interface exhibited a weakly convex morphology. With continued solidification, the interface transitioned to a planar configuration and subsequently evolved into a convex morphology toward the end of growth. This evolution occurred while maintaining complete detachment from the container wall.

Within the investigated growth-rate range (2. 5mm·h^{-1}), no cellular or dendritic interface breakdown was observed. The interface remained smooth and stable throughout growth, indicating effective suppression of gravity-driven instabilities.

Figure 5, the X-ray diffraction measurements confirmed single-crystalline growth with dominant (220) or (111) orientations, depending on growth conditions. The full width at half maximum of the rocking curves was typically below 128 arcsec Table 2-3. Energy-dispersive X-ray (EDX) spectroscopy measurements showed axial compositional uniformity within at. 2%, while radial compositional variation remained below the detection limit within experimental uncertainty. These values place conventional growth systems in the gravity-dominated region of the stability map. XRD peaks of 95% detached as grown ingots were showed (111) and (220) diffraction by the very sharp peaks with orientation (plane) of the (111) and (110) of detached crystals are shown in Fig.6. The growth of a seed was not serendipitously or spontaneously, but it is due to an ampoule geometry and thermal condition at the initial growth, where at low-energy planes were under greater capillary pressure than the hydrostatic pressure with a stable vacuum gap and temperature gradient. The meniscus acquired orientation showed entire crystal grows fully detached, and transport becomes diffusion-dominated, alike a microgravity-equivalent physics.

Table 2, the thermal and process parameters, the core experimental conditions defining seed formation, detachment, and entirely directional solidification parameters, and physical measurements of several detached ingot grown in VDS process are shown for easy consideration, comparison, and interpretation. The italic figures in bracket shows number of growths runs repeated in VDS process for improvement of highest crystallization.

Sr No. ⇓ ⟹ Crystal Properties	InSb ***(18)***	InSb:Te ***(4)***	InSb:Bi ***(4)***	GaSb ***(6)***	GaSb:Te ***(4)***	GaSb:In ***(4)***	InSb:Ga ***(5)***	$In_{0.5}G_{0.5}Sb$ ***(10)***
1 In (gms)	9.68	9.72	9.57			0.66	2.62	2.98
2 Ga(gms)				20.95	6.8	3.61	4.76	11.21
3 Sb(gms)	10.24	10.28	10.37	37.16	11.2	7.0	11.12	4.82
4 Dopant(gms)		0.35 x 10^{-3}	0.05		0.38 x 10^{-3}	0.15%	0.25%	0.5%
5 Set Temp (^{0}C)	800	820	800	850	810	850	850	850

6	Growth Temp (^{0}C)	575	575	575	762	762	762	762	762
7	Gradient (^{0}C. cm^{-1})	10-32	10-32	10-32	10-32	10-32	10-32	10-32	10-32
8	Up/Down rate (mm/h)	5	5	2	5	5	5	5	3
9	Rotation speed (rpm)	10	10	10	10	10	10	10	10
10	Cone angel (0^0)	54	57	58	62	664	74	65	72
11	Gap width (µm)	69	112	73	95	128	139	151	145
12	Crystal length (mm)	62	60	58	75	66	42	52	49
13	Crystal dia. (mm)	12	12	10	22	18	10	14	12
14	FWHM (arcsec)	65	87	95	49	98	95	112	128
15	Refl / Orient (Laue/Raman)	220 /110	220 /110	220 110	220 /110	220 /110	220/110	220 /110	220 /110
16	Energy gap (eV)	0.16	0.18	0017	69	0.73	0.51	0.79	0.46
17	Mobility µ 10^3(cm^2/V.sec)	60	26.9	44.5	1.12	0.12	4.96	3.26	1.1
18	Resistivity 10^{-3} (Ohm.cm)	3.02	0.41	0.52	4.45	5.25	1.94	7.78	3.18
19	Hall Coeff. R_H (cm^3/Coulomb)	-165	-10.6	22.42	5.57	- 6.16	- 7.06	-7.21	3.81
20	Carrier Conc. 10^{17}(cm^{-3})	0.38	5.8	6.1	2.1	16.6	88.6	86.8	81.1
22	Dislocation 10^3 (cm^{-2})	0.62	2.3	2.4	0.67	1.4	3.91	2.29	1.2
23	Micro-Hardne (GPa)	2.25	2.1	2.15	4.42	4.12	3.98	3.85	3.72
24	Crystal growth	Entire detached	Entire detached	Entire detached	Entire detached	Entire detached	Entire detached	Entire detached	Entire detached

25	Semicon. type	Comple x	n-type	n-type	p-type	n-type	n-type	n-type	complex

Note: The black italic figures in brackets are number of growths runs for an entire detached crystals by VDS process on terrestrial conditions. Crystals grown - InSb:Bi ***(7)***, InSb:N ***(5),*** InSb:Se ***(3)***, GaSb:Mn ***(3)***, GaSb: Mg ***(2)***, and $Ga_{(1-X)}In_X$ Sb (8)**,** these crystals were grown by research scholars using VDS process since 1994 (Gadkari et.al. 2012 to 2020, 2025). Thermal and process parameters used in VDS Growth process, the core experimental conditions defining seed formation, detachment, and entirely directional solidification parameters.

XRD patterns of the middle-solidified region of the detached ingots (a) InSb, and (b) GaSb, revealing dominant (111) for InSb, and (110) for GaSb diffraction pattern, planar growth of entire detached crystal also revealing dominant (220) diffraction pattern, and (110) orientation plane growth. This confirms self-generated crystallographic seed orientation emerging from interfacial energy minimization prior to full directional growth. The 95% frown ingot In VDS showed the dominant diffraction patterns with (111), and (110) orientation. It indicates that evolution of the self-oriented seed during initial crystallization. Sequential thermal stages, it processes as melting → supercooling → nucleation → orientation establishing. Meniscus curvature stabilizes seed orientation via Young–Laplace pressure. The X-Ray diffraction pattern shows single crystal detached growth. Growth continuation from the self-oriented seed, showing propagation of orientation along the entire 42–75 mm detached crystal length. No evidence of lattice tilting or rotation due to absence of wall-induced torque Table 2-3.

Table-3 Thermal and process parameters used in VDS Growth process, the core experimental conditions defining seed formation, detachment, and entirely directional solidification parameters.

Sr. No.	Crystal	GaSb-2	GaSb-4	GaSb:In-1 In = 0.5	GaSb:In-2 In = 0.25	GaSb:In-3 In = 0.15
1	Source Ga (gms)	6.41	20.95	2.92	4.76	3.61
	Sb (gms)	11.21	37.16	10.21	11.12	7.00
	Dopant In (gms)	--	--	4.82	2.62	0.66
2	Setting temperature (0^0c)	850	850	850	850	850
3	Growth Temperature (0^0c	760	760	760	760	760
4	Freezing rate (0^0C/ cm)	32	32	32	32	32
5	Up/Down Rate (mm/hr)	5	5	5	4	4
6	Rotational Speed (rpm)	10	10	10	10	10
7	Cone Angle (0^0)	55	60	72	65	74
8	Gap width (µm)	135	135	145	151	139
9	Crystal length (mm)	45	62	50	52	42
10	Crystal diameter (mm)	16	20	12	14	10
11	FWHM (arcsec)	95	95	158	147	126

12	Orientation (XRD),/Raman	220	220	220	220	220
13	Energy gap (Eg)(eV)	0.69	0.69	0.46	0.49	0.51
14	Mobility10^3 (cm^2 / Vcsec)	1.06	1.12	1.084	9.26	3.64
15	Resistivity 10^{-3} (Ohm-cm)	3.56	4.45	3.18	7.78	1.94
16	Hall effect (cm^3/ Coulomb)	3.78	5.57	3.44	72.1	- 7.06
17	Carrier Concen10^{18} (cm^{-3})	0.27	0.21	1.81	8.68	8.86
18	Argon pressure (torr)	250	260	242	250	275
19	Disloc density x10^3 (cm^{-2})	0.96	0.96	1.2	4.9	8.9
20	Micro-Hardness H_v (GPa)	4.42	4.42	3.72	3.85	3.98
21	Crystal Growth	Detached	Detached	Detached	Detached	Detached
22	Type of Semiconductor	p	p	complex	p	n

Figure 6, (a) The Laue back-reflection analysis confirms that crystals grown by the VDS process exhibit true single-crystalline order, evidenced by sharp, unsplit diffraction spots and the absence of diffuse scattering. This indicates that crystallization proceeds under a stable, orientation-preserving crystal–melt interface, despite the presence of terrestrial gravity. In the VDS configuration, a capillary-supported meniscus forms between the melt and the ampoule wall. The dominant restoring force at the interface is the Laplace pressure,

$\Delta Pc = \gamma (1/R1+1/R2)$

which exceeds the hydrostatic pressure perturbation, thereby suppressing gravity-driven interface distortion and melt convection. This capillary dominance enforces a self-centered, detached growth front, minimizing wall contact and eliminating heterogeneous nucleation sites.

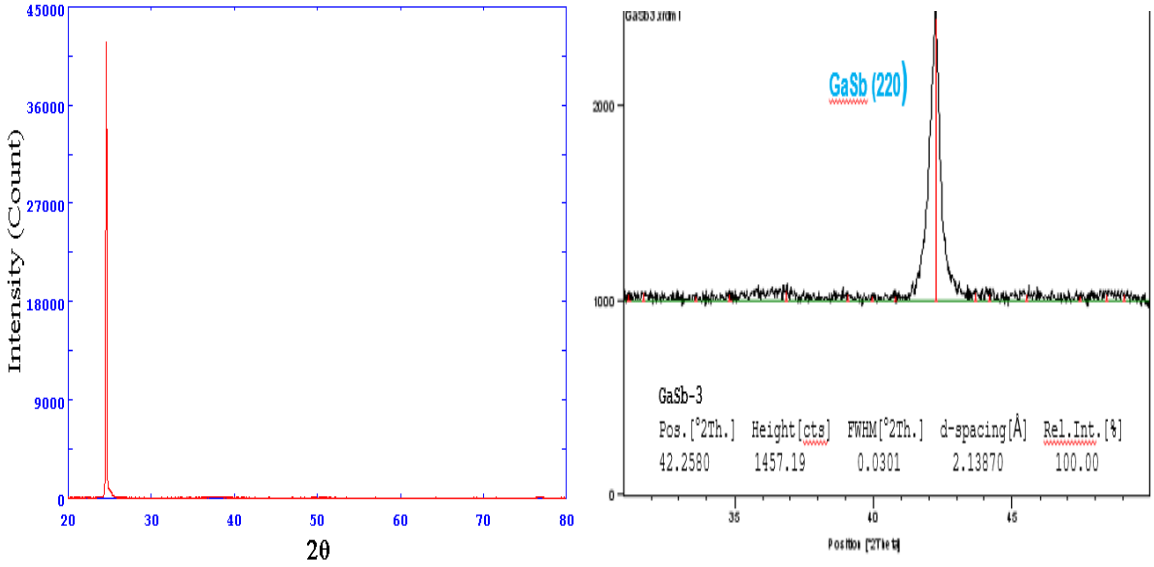

(a) (b)

Fig. 5(a-b) the sharp peaks of XRD patterns of the substates cut from middle of the as grown detached ingots, (a) InSb, and (b) GaSb XRD back diffraction patterns, where planar interface growth was active.

Figure 6(b) The Vickers microhardness measurements further reveal mechanical homogeneity and low defect density, as indicated by uniform hardness values and crack-free indent morphology along both axial and radial directions. Since microhardness is highly sensitive to dislocation density and residual stress, the observed uniformity directly reflects stress-free solidification enabled by capillary stabilization.

Figure 7, the reconstructed by post-growth Etch-pit density (EPD) mapping along the crystal length showing values of $0.62x10^3$ – 8.9×10^3 cm^{-2} Table 2-3, matching microgravity-grown III–V crystals. Reduced thermal stress and absence of wall shear contribute to low defect densities. Microstructure and EPD: Etch pits have a shape that is characteristic of the crystallography of the etched surface, they form equilateral triangles on cube edge on (110) planes in(a-b), the coalscences growth (c) during solidification reveals minor disturbance during growth into melt, while, (d) the small angle phase change solidification at interface front, and (e) a lamellae growth reveals crystallographic growth due to capillary effect. Chemical etching revealed dislocation densities in the range of 10^3–10^4 cm^{-2}, significantly lower than those commonly reported for container-contact growth in 1g.

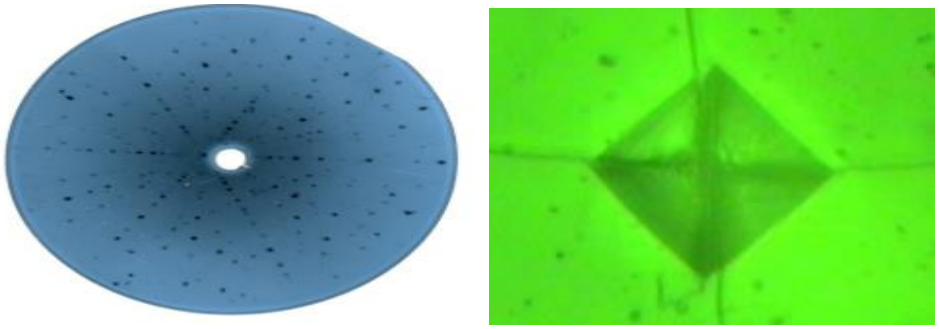

(a) (b)

Fig. 6(a) the back scattered Laue pattern of GaSb, and (b) Vikar microhardness test for InSb indicate also the enhanced crystallization as an added test to confirm the growth in VDS process, the values of microhardness are reported in Table 2-3

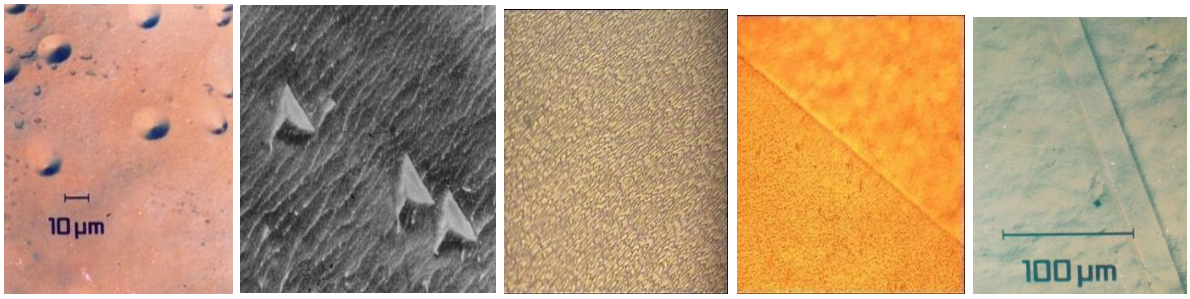

(a) (b) (c) (d) (e)

Fig.7 reveals the gorowth morphology during the soilidification process (a) the circular EPD, (b) the triangular (110) oriented eatch pits, (c) the coalscences, (d) the uniform straight phase growth (boundary line), and (e) the lamallae straight growth by detached solidification, EPD details in Table 2-4, the segregation redistribution and EPD Table 2-3

"The experimental detached growth by VDS process and all characterizations, together, these results demonstrate that capillary forces in the VDS process enhanced crystallization by stabilizing the crystal–melt interface, suppressing gravity-induced instabilities, and reducing thermomechanical stress, leading to structurally perfect and mechanically uniform bulk crystals under 1g conditions".

Ingots solidification under 1g

This can be divided into two types of regimes, where Regime-A, the solidification in contact with inner wall of ampoule, and Regime-B, the solidification wall de-coupled.

The observations motivate the formulation of a quantitative criterion capable of distinguishing Regime-A (gravity-influenced, wall-contact growth) from Regime-B as below.

Regime B: Wall-Decoupled Solidification (Capillary-Dominated Growth): In Regime-B, the melt and the growing crystal are not in mechanical contact with the container wall over a substantial portion of the growth length. This regime has been experimentally realized and repeatedly observed in the VDS process under terrestrial gravity, where a continuous gas-filled gap is maintained between the crystal and the ampoule wall throughout growth. Since the 1994s, VDS experiments on Sb-based semiconductor systems have consistently demonstrated entirely detached growth under 1g conditions, verified by the post-growth sectioning.

In VDS, the absence of wall contact removes the no-slip boundary condition and decouples the melt from direct gravitational forcing through viscous shear. As a consequence, the stability of the melt column and the crystal–melt interface is governed primarily by capillary pressure arising from interface curvature, rather than by buoyancy-driven convection. Characteristic features of this regime observed in VDS include suppressed radial transport, stable interface morphologies, and significantly reduced defect densities compared with conventional wall-contact growth.

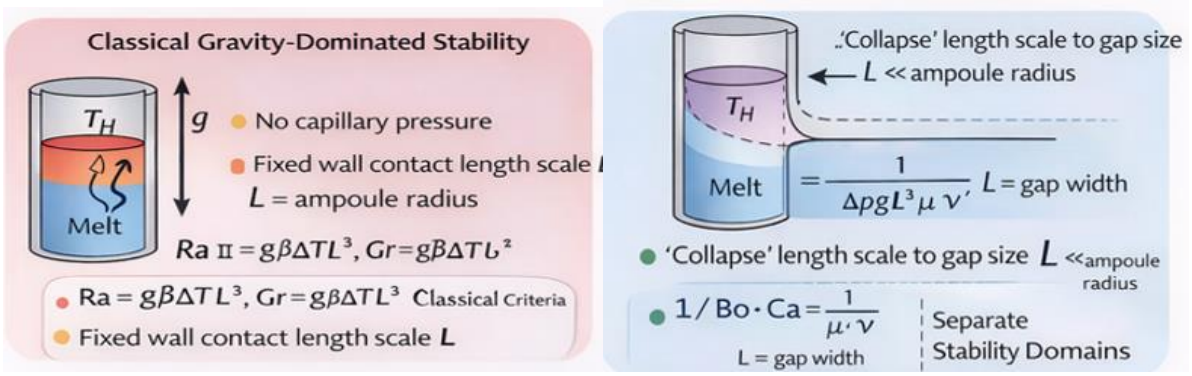

(a) Resume-A (b) Resume-B

Fig. 8 (a) Why classical criteria cannot predict detached growth (b) Capillary-dominated stability (entirely detached growth

A defining experimental signature of Regime B in VDS is the reproducible evolution of the crystal–melt interface from concave to planar and finally to convex morphology while remaining fully detached from the container wall. This behaviour is incompatible with classical gravity-dominated solidification models but is consistent with a capillary-stabilized interface governed by the Young–Laplace pressure balance. Improvements in crystallographic orientation, low etch-pit densities, and enhanced compositional uniformity further confirm the mechanical and thermal decoupling achieved in VDS.

Independent support for capillary-dominated detached growth under terrestrial gravity is provided by dewetted Bridgman experiments, where a gas-filled gap forms between the crystal and crucible wall. Duffar and co-workers demonstrated that stable detached growth can be sustained when surface-tension forces at the meniscus exceed gravity-induced hydrostatic pressure (Duffer et.al. 2000). Subsequent experiments on InSb, CdTe, and Ge systems confirmed that detached growth reduces wall-induced stress and improves crystal quality, consistent with VDS observations (Duffer et.al 2009; Mazuruk, et.al. 2013; Balint et.al 2012) Analytical and numerical investigations of dewetted growth established that meniscus shape and stability are governed by the Young–Laplace relation, and that detached configurations remain stable when capillary pressure dominates gravitational loading (Yu et.al 2019; Schwabe et.al. 2002; Shevtsova et.al 2003). These studies provide a theoretical foundation for the experimental behaviour observed in VDS but do not explicitly address the sustained axial stability achieved in the VDS configuration.

Microgravity directional solidification experiments offer a complementary benchmark for Regime-B behaviour. Under reduced gravity, buoyancy-driven convection is strongly suppressed, leading to diffusion-dominated transport, stable planar or weakly curved interfaces, and improved compositional homogeneity (Kakimoto et.al 2005; Tourret et.al. 2015; Medjkoune et.al. 2025). Notably, the interface morphologies, transport characteristics, and defect densities reported in microgravity experiments closely resemble those observed in VDS detached growth under terrestrial gravity (Volz et.al. 2011).

Despite the long-standing experimental evidence of entirely detached growth in VDS, classical solidification theory has not explicitly distinguished this capillary-dominated regime from gravity-influenced wall-contact growth. Most conventional formulations implicitly assume mechanical coupling

between the melt and the container wall, embedding gravity into the governing transport equations. As a result, the VDS detached growth regime remained unformulated as a distinct stability domain.

These observations motivate the formulation of a quantitative criterion capable of distinguishing Regime-A (gravity-influenced, wall-contact growth). Despite this experimental evidence, classical solidification theory has not explicitly distinguished Regime-B from gravity-dominated wall-contact growth. Most conventional formulations implicitly assume mechanical coupling between the melt and the container wall, thereby embedding gravity into the governing transport equations. As a result, the capillary-dominated detached regime has remained "unformulated as a distinct stability domain".

Regime B (capillary-dominated, wall-decoupled growth). This requirement leads directly to the *Gadkari Detached Stability Criterion (GDSC)*, introduced in the following section.

Numerical Evaluation of the Gadkari Detached Stability Criterion

In contrast, characteristic parameters for conventional wall-contact growth yield significantly larger effective transverse length scales, resulting in Bond numbers approaching unity. To quantitatively distinguish Regime-A (wall-contact, gravity-influenced growth) from Regime B (wall-decoupled, capillary-dominated growth), the *Gadkari Detached Stability Criterion (GDSC)* is evaluated using experimentally relevant parameters. The GDSC is defined as:

$$GDSC = 1/\ Bo\ Ca$$

where the Bond number (Bo and Capillary number (Ca) are given by

I) $Bo = \Delta\rho\, g\, L^2/\sigma$ II) $Ca = \mu\, v/\sigma.$ III) $GDSC = \sigma^2/\Delta\rho\, g\, \mu\, v\, L^2$

Here, $\Delta\rho$ is the density difference between crystal and melt, g is gravitational acceleration, L is the characteristic transverse length scale (gap or contact length), σ is surface tension, μ is melt viscosity, and v is the growth velocity.

Regime-A: Conventional Wall-Contact Growth

Using experimentally measured gap widths, growth rates, and material properties, the Bond and Capillary numbers were evaluated for VDS growth conditions., placing all VDS experimental points deep within the capillary-dominated regime, the parameters used from Table 4. For conventional Bridgman or VGF growth, the melt remains in contact with the container wall.

The relevant transverse length scale is therefore the ampoule radius, typically:

$L \sim 5\times10^{-3}$ m, $\Delta\rho \sim 500$ kg m^{-3}, $\sigma \sim 0.5$ N m^{-1}, $\mu \sim 2\times10^{-3}$ Pa.s, and $v \sim 1\times10^{-6}$ m s^{-1}. This yields:

$$Bo\text{-}A = 500\times9.81\times (5\times10^{-3})^2/0.5 \approx 0.25,$$

$$Ca\text{-}A = 2\times10^{-3}\times1\times10^{-6}/0.5 \approx 4\times10^{-9}$$

$$\Rightarrow GDSC\text{-}A = 1/\ Bo\text{-}A\ Ca\text{-}A \approx 1\times10^{9}$$

Although GDSC-A is numerically large, this value is misleading, because in Regime-A the interface is mechanically constrained by wall contact. The no-slip boundary condition enforces viscous coupling and enables buoyancy-driven convection, invalidating capillary stabilization despite a formally large GDSC. Thus, GDSC is not physically operative when wall contact exists. This highlights a crucial point: GDSC applies only when wall contact is absent.

Regime-B: VDS Entirely Detached Growth

In the VDS process, the melt and crystal are decoupled from the container wall by a stable gas-filled gap. The relevant transverse length scale is therefore the measured gap width, not the ampoule radius. Typical experimental values measured in VDS are:

Gap width: $L \sim 1\times10^{-4}$ m (100μm), $\Delta\rho \sim 500\ \mathrm{kg\,m^{-3}}$, $\sigma \sim 0.5\ \mathrm{N\,m^{-1}}$, $\mu \sim 2\times10^{-3}$ Pas, $v \sim 3\times10^{-7}\ \mathrm{m\,s^{-1}}$v. This yields:

$\text{Bo-B} = 500\times9.81\times(1\times10^{-4})^2/0.5 = 1\text{x}10^{-4}$,

$\text{Ca-B} = 2\times10^{-3}\times3\times10^{-7}/0.5 \approx 1.2\times10^{-9}$

$\Rightarrow \text{GDSC-B} = 1/\text{Bo-B Ca-B} \approx 8\times10^{12}$

Physical Interpretation

The comparison reveals a fundamental distinction: Regime- A (wall-contact): Gravity couples directly to the melt via the wall, Convection dominates transport, Capillary stabilization is ineffective, Classical gravity-based criteria apply.

Regime-B (VDS detached growth: Wall coupling is eliminated, Transverse length scale collapses from mm to μm, Bo ≪ 1, Ca ≪ 1, Capillary pressure dominates gravity, Transport becomes diffusion-controlled.

In Regime-B, the extremely large value of GDSC reflects a true physical dominance of capillarity, the formal numerical artifact. This explains why entirely detached growth can be sustained under full terrestrial gravity in the VDS process.

Resolution of the Long-Standing Detachment Paradox

Entirely detached growth in VDS has been experimentally observed since the 1994s, yet remained unexplained within classical solidification theory. The numerical evaluation presented here resolves this paradox by demonstrating that: 1. Wall decoupling fundamentally changes the governing force balance. 2. The relevant length scale shifts from ampoule radius to gap width. 3. Capillary pressure overwhelms gravity-driven instabilities. 4. VDS operates in a capillary-dominated stability regime.

The *Gadkari Detached Stability Criterion* therefore provides the missing quantitative framework that explains why VDS behaves as a microgravity-equivalent solidification system under 1g.

Regime A: Wall-Contact Solidification (Gravity-Influenced Growth)

In conventional crystal growth methods such as Bridgman, Vertical Gradient Freeze (VGF), and Czochralski growth, the melt and the growing crystal remain in continuous contact with the container wall.

This contact enforces a no-slip boundary condition, which directly couples gravity to the melt through viscous shear. Under these conditions: 1. Buoyancy-driven convection is unavoidable. 2. Hydrostatic pressure acts directly on the melt column. 3. Radial temperature and solute gradients develop. 4. Transport is inherently three-dimensional.

The governing physics of this regime is well established and described by classical dimensionless numbers and stability criteria, including: Rayleigh number (Ra) – buoyancy-driven convection, Grashof number (Gr) – gravity–viscous balance, Péclet number (Pe) – advection–diffusion coupling, Mullins–Sekerka criterion – interface, morphological stability, and Scheil relation and solutal diffusion laws.

These formulations implicitly assume wall contact and gravity coupling. As a result, gravity-driven convection dominates transport, and the role of capillarity is limited to local interface smoothing. This regime (Regime A) is therefore gravity-influenced and convection-dominated by construction.

Regime-B: Wall-Decoupled Solidification (Capillary-Dominated Growth)

In contrast, experimental observations in the VDS process reveal a second regime in which the melt and crystals are not in mechanical contact with the container wall over the growth length. In this regime: A continuous gas-filled gap exists between crystal and wall, The no-slip boundary condition is removed, Hydrostatic pressure is not directly transmitted to the interface, and Melt stability is governed by interface curvature and surface tension.

Here, the dominant restoring force is capillary pressure, not gravity. The crystal–melt interface is stabilized by the Young–Laplace pressure balance, and transverse transport is strongly suppressed. Transport becomes predominantly axial and diffusion-controlled, even under terrestrial gravity.

This regime (Regime B) exhibits characteristics traditionally associated with microgravity solidification: Suppressed buoyancy-driven convection, Stable planar or weakly curved interfaces, reduced radial segregation, and improved crystallographic quality.

Importantly, this regime has not been explicitly formulated or quantified in classical solidification theory, because conventional models implicitly assume wall contact and gravity coupling.

Why Regime-B Was Not Reported Earlier

The absence of a formal description of Regime-B in the literature arises from two implicit assumptions in classical models:

1. Wall contact is unavoidable under 1g conditions
2. Gravity always dominates over capillarity at macroscopic scales

The VDS process violates both assumptions simultaneously. By enabling sustained wall decoupling and stabilizing the melt column through capillary pressure, VDS accesses a previously unformulated solidification regime under terrestrial gravity.

Experimental evidence of entirely detached growth in VDS has existed since the 1994s; however, without a dedicated dimensionless framework, these observations could not be reconciled with classical gravity-based descriptions.

Formulation of the Gadkari Detached Stability Criterion (GDSC)

To quantitatively distinguish Regime-A from Regime-B, a dimensionless criterion is required that directly compares capillary stabilization against gravity-driven destabilization at the solid–liquid interface**.**
The Gadkari Detached Stability Criterion (GDSC) is formulated as:
GDSC = 1/Bo Ca

Bond number: Bo =$\Delta\rho$ g L^2/σ represents the ratio of gravity to capillary forces,

Capillary number: Ca = μ v/σ represents the ratio of viscous forces to capillary forces,
Where, $\Delta\rho$ is the density difference, g is gravitational acceleration, L is the characteristic gap/interface length scale, σ is surface tension, μ is melt viscosity, v is the growth velocity.

Figure 9. White open circles (○): → Conventional wall-contact growth (Regime A)- Bridgman / VGF / container-contact systems, Melt is in mechanical contact with the ampoule wall, Gravity directly couples to the melt, Buoyancy-driven convection dominant, Data points lie in high Bo and/or high Ca region. These points represent classical gravity-influenced solidification, where capillary stabilization is ineffective. Green filled circles (●): → VDS experimental points (Regime B) has Entirely detached growth observed, melt not in contact with the wall, Capillary pressure dominates gravity, Stable detached interface under 1g, Points lie deep in low Bo – low Ca region, and these are the key experimental results of your work. Green squares (■): → Dewetted Bridgman experiments (literature) has Partial or complete detachment reported, Capillary-assisted growth under 1g, serve as independent experimental support, located near the VDS region but typically less deep, and these show that capillary-controlled detachment is not unique, but VDS stabilizes it more strongly. Yellow triangles (▲): → Microgravity directional solidification data (literature) has Reduced gravity conditions, Diffusion-dominated transport, Minimal convection, Interface morphologies similar to VDS, and these points provide the benchmark reference showing that VDS approaches microgravity behavior without reducing g. *The solid curve represents the critical boundary defined by the Gadkari Detached Stability Criterion, Bo.Ca = constant, separating gravity-influenced wall-contact growth from capillary-dominated entirely detached growth.*
Figure 9. Stability map of the Bond number–Capillary number, it demonstrates the *Gadkari Detached Stability Criterion,* in this diagram, the filled symbols (green, blue, yellow) represent VDS experiments exhibiting entirely detached growth under terrestrial gravity, while open symbols (white) correspond to conventional wall-contact growth. The capillary-dominated region (low Bo, low Ca) represents a gravity-resistant solidification regime. In this Stability map, the solid curve (black line) represents the critical boundary defined by Bo Ca = const, separating gravity-influenced wall-contact growth from capillary-dominated entirely detached growth. Open symbols (white) correspond to conventional wall-contact crystal growth systems, while filled symbols represent VDS experiments exhibiting sustained entirely detached growth under terrestrial gravity. Squares indicate dewetted Bridgman growth reported in literature, and triangles correspond to microgravity directional solidification experiments. Further, it (Fig. 9) presents a dimensionless stability map that unifies experimental observations of crystal growth under terrestrial gravity and microgravity within a.

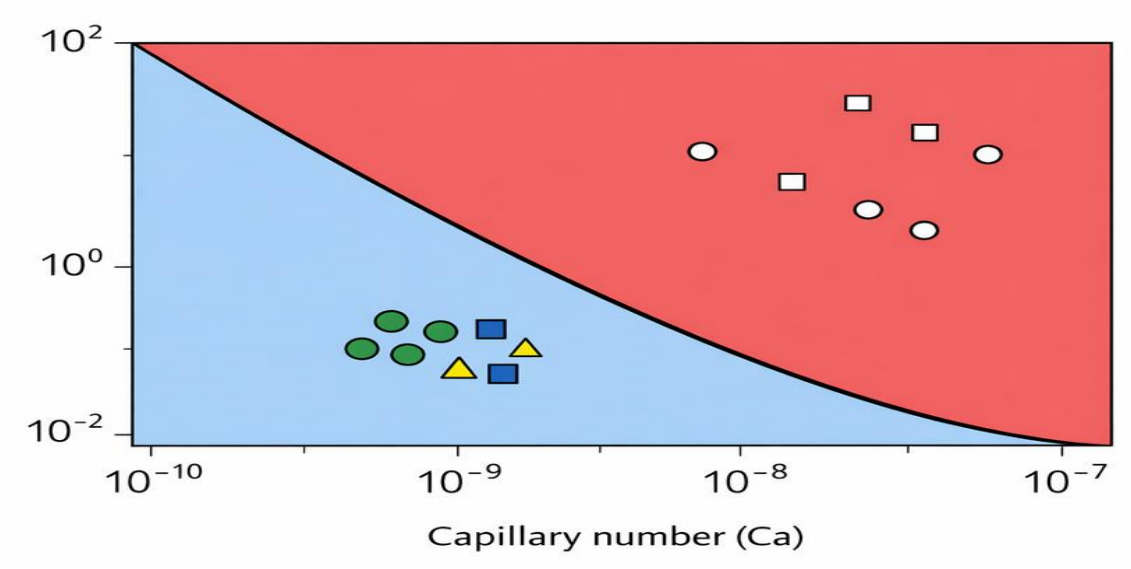

Fig. 9 The represents Capillary number Vs Bond number. The solid curve represents the critical boundary defined by the *Gadkari Detached Stability Criterion*, Bo Ca = constant, separating gravity-influenced wall-contact growth from capillary-dominated entirely detached growth. It is shown as the black bold curve line. Symbols: Open circles—conventional wall-contact growth; filled circles—VDS experiments exhibiting entirely detached growth; squares—dewetted Bridgman growth reported in literature; triangles—microgravity directional solidification experiments.

single physical framework. The axes represent the Bond number (Bo), quantifying the ratio of gravitational to capillary forces, and the Capillary number (Ca) quantifying the ratio of viscous to capillary forces. Together, these parameters characterize the competition between gravity-driven destabilization and surface-tension-driven stabilization at the crystal–melt interface.

The solid curve (black) corresponds to the critical condition Bo Ca = constant, which defines the *Gadkari Detached Stability Criterion*. This boundary is not an empirical fit but a physics-based threshold derived from force-balance considerations. It separates two fundamentally different solidification regimes. Data points (red) located above or to the right of the curve correspond to gravity-influenced, wall-contact growth, where buoyancy-driven convection and viscous coupling dominate transport and interface stability. These conditions are characteristic of conventional Bridgman and Vertical Gradient Freeze growth methods.

In contrast, data (blue) points located below and to the left of the curve lie in the capillary-dominated regime, where surface tension overwhelms gravitational and viscous effects. The VDS experimental points cluster deep within this region, demonstrating that entirely detached growth under terrestrial gravity is achieved when wall contact is eliminated and the relevant transverse length scale collapses from the ampoule radius to the micrometer-scale gap width. Under these conditions, transport becomes diffusion-controlled and interface stability is governed by capillary pressure rather than by gravity.

The proximity of dewetted Bridgman data to the VDS region confirms that capillary-assisted detachment under 1g is physically plausible but typically less stable without the specific VDS configuration. Microgravity experimental points occupy a similar region of the map, providing an

independent benchmark and demonstrating that VDS reproduces key features of microgravity solidification without reducing gravitational acceleration.

Overall, the stability map provides quantitative evidence that the VDS process operates in a distinct capillary-dominated solidification regime. The Gadkari Detached Stability Criterion thus resolves the long-standing question of sustained entirely detached growth under terrestrial gravity and establishes a direct physical link between VDS and microgravity-equivalent solidification behavior.

Physical Interpretation of GDSC

GDSC ≪ 1

→ Gravity and viscous effects dominate
→Wall-contact growth
→Convection-driven transport
→ Regime-A (classical solidification)

GDSC ≫ 1

→ Diffusion-controlled transport
→ Stable wall decoupling
→ Capillary pressure dominates
→ Stable wall contact

Experimental conditions in the VDS process consistently yield GDSC values much greater than unity, explaining the observed persistence of entirely detached growth under terrestrial gravity.

Discussion

The results demonstrate that entirely detached crystal growth under terrestrial gravity represents a distinct capillary-dominated solidification regime. Figures 10–11 collectively show that when wall contact is eliminated, gravity no longer governs interface stability through buoyancy-driven convection. Instead, capillary pressure dominates the force balance at the crystal–melt interface. Classical gravity-based criteria such as the Rayleigh and Grashof numbers remain valid for wall-contact growth (Regime-A) but are not applicable to wall-decoupled growth. The *Gadkari Detached Stability Criterion* captures the governing physics of Regime-B by explicitly incorporating capillary effects and the relevant micrometer-scale length associated with the crystal–wall gap. The clustering of VDS experimental data deep within the capillary-dominated region of the stability map, together with the overlap with microgravity solidification data, demonstrates that VDS reproduces key microgravity-like features without reducing gravitational acceleration. This resolves the long-standing question of sustained detached growth in VDS and establishes capillary control as the primary mechanism enabling gravity-resistant solidification under 1g conditions.

The conventional classical wall contacts and capillary pressure solidification

Taken together, figures provide a unified experimental and physical picture of solidification under terrestrial gravity. Which establishes the classical gravity-dominated framework. As schematically (below) in figures, this wall contact enforces a no-slip boundary condition, directly coupling gravitational body forces to the melt and promoting buoyancy-driven convection. In contrast, the VDS process operates in a fundamentally different configuration. Conventional solidification processes under terrestrial gravity

are characterized by continuous mechanical contact between the melt and the container wall. Demonstrates the experimentally realized wall-decoupled configuration unique to the VDS process. Where, the growing crystal and melt are separated from the container wall by a stable gas-filled gap, resulting in wall-decoupled solidification under full terrestrial gravity (below figures).

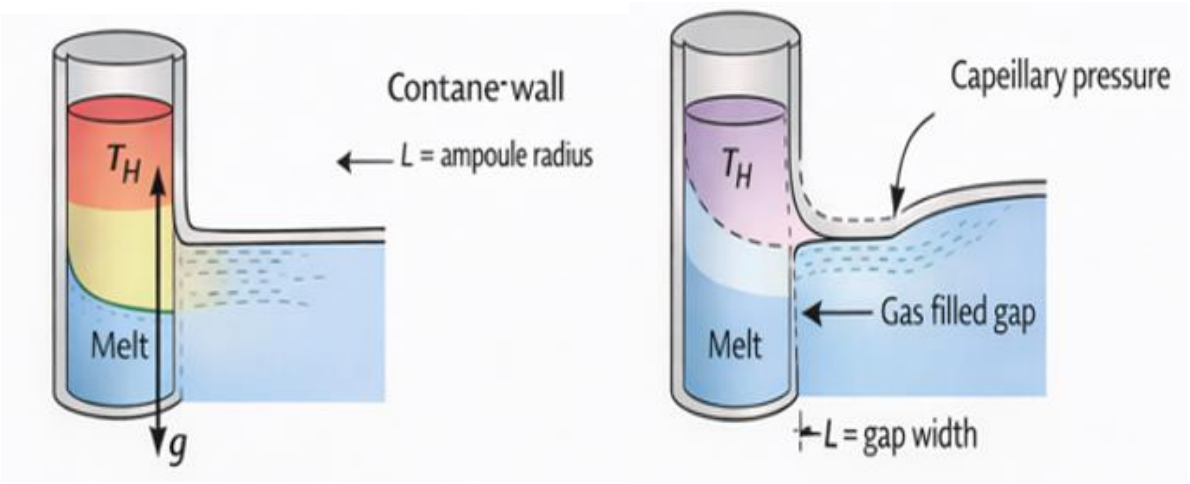

(a) (b)

Figure 10(a) Regime-A, schematic of classical wall-contact crystal growth under terrestrial gravity. The melt remains in continuous mechanical contact with the container wall, enforcing a no-slip boundary condition and enabling gravity-driven convection. **Figure 10(b) Regime-B, s**chematic of the VDS wall-decoupled process exhibiting entirely detached growth. A stable gas-filled gap separates the crystal–melt interface from the container wall, resulting in wall-decoupled solidification under terrestrial gravity.

Classical wall-contact solidification (Regime A): Figure 10(a) represents the classical solidification configuration in which the melt remains in continuous contact with the container wall. Under these conditions, gravitational body forces are transmitted directly to the melt through viscous coupling at the wall, leading to buoyancy-driven convection and three-dimensional transport. Classical gravity-based criteria, including the Rayleigh and Grashof numbers, are therefore applicable and successfully describe flow onset and convection intensity in such systems. However, these criteria implicitly assume wall contact and do not address the stability of the crystal–melt interface when mechanical coupling to the container is removed. Figure 10(a) illustrates the conventional solidification configuration used in Bridgman, Vertical Gradient Freeze, and related terrestrial growth techniques. Mechanical contact between the melt and the container wall couples gravitational body forces directly to the melt through viscous shear. The characteristic transverse length scale is the ampoule radius, over which hydrostatic pressure and buoyancy act. Under these conditions, transport is inherently three-dimensional and dominated by buoyancy-driven convection. Classical stability criteria such as the Rayleigh and Grashof numbers are applicable in this regime because gravity is directly transmitted to the melt through wall contact.

VDS wall-decoupled solidification (Regime B): In contrast, the VDS configuration shown in Fig. 10(b) eliminates wall contact over a substantial the growth length by maintaining a stable gas-filled gap between the crystal and the ampoule wall. This wall decoupling suppresses viscous coupling and prevents direct transmission of gravitational forces to the melt. As a result, the relevant transverse length scale governing

stability collapses from the ampoule radius to the micrometer-scale gap width. Experimental evidence confirms that under these conditions, the crystal–melt interface remains stable and entirely detached throughout growth, despite the presence of full terrestrial gravity. Figure 10 (b) depicts the VDS configuration in which the growing crystal and melt are mechanically decoupled from the container wall by a continuous gas-filled gap. The absence of wall contact removes the no-slip boundary condition and prevents direct transmission of gravitational forces to the melt through viscous coupling. The relevant transverse length scale collapses from the ampoule radius to the micrometer-scale gap width. Under these conditions, interface stability is governed primarily by capillary pressure rather than by gravity-driven convection, enabling sustained entirely detached growth under 1g conditions.

Figure 11(a) clarifies the conceptual separation between these regimes, and Fig. 11(b) provides the quantitative stability criterion that explains why entirely detached growth can be sustained under 1g conditions. The results presented in this work demonstrate that entirely detached crystal growth under terrestrial gravity is not an anomalous or transient phenomenon, but the manifestation of a distinct capillary-dominated solidification regime. The combined experimental observations, schematic representations, and dimensionless analysis establish that the governing physics of the VDS process fundamentally differs from that of conventional wall-contact growth systems.

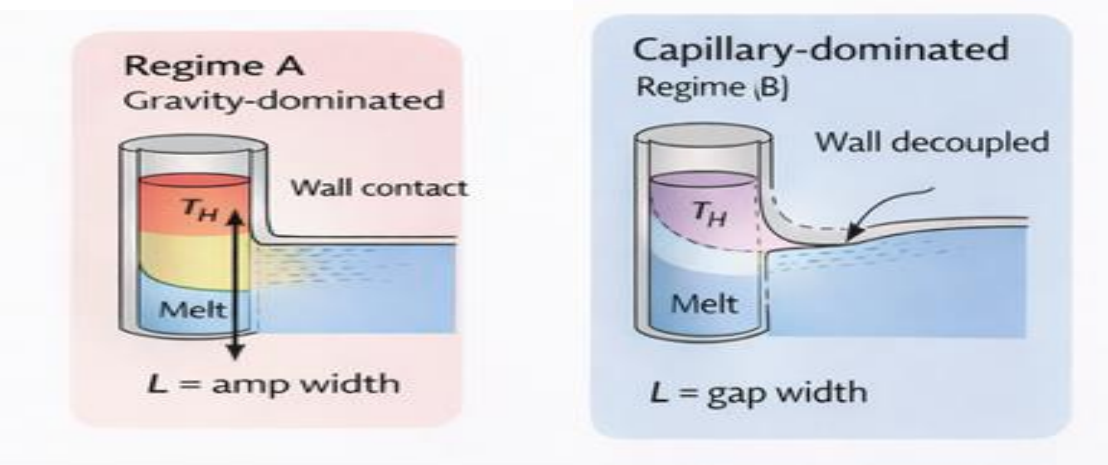

(a) No meniscus (b) With meniscus

Figure 11 experimental Observations and regime identification, the elimination of wall contact in VDS fundamentally alters the governing transport and stability mechanisms. A conceptual comparison between the two growth configurations is presented in Fig. 11(a), which highlights the distinction between gravity-influenced wall-contact growth (Regime A) and capillary-dominated wall-decoupled growth (Regime B) Fig-11(b). Experimental observations obtained in the VDS process consistently fall within Regime B, characterized by suppressed transverse transport, stable interface morphologies, and sustained entirely detached growth over extended lengths

Dimensionless Analysis / GDSC regime

The quantitative separation of the two solidification regimes is summarized in the stability map shown in Fig. 12. This map plots the Bond number against the Capillary number and introduces the *Gadkari Detached Stability Criterion* as the stability boundary separating gravity-influenced and capillary-

dominated growth regimes. Data corresponding to conventional wall-contact growth cluster in the gravity-dominated region of the map, whereas VDS experimental points lie deep within the capillary-dominated domain. Dewetted Bridgman and microgravity data occupy intermediate and overlapping regions, demonstrating that VDS reproduces key microgravity-like features under terrestrial conditions.

Figure 12 (a) summarizes the conceptual separation between these two regimes. Regime A corresponds to gravity-influenced wall-contact growth, where convection dominates transport and interface stability is governed by classical criteria. Regime-B Fig- 12 (b) corresponds to wall-decoupled growth, where capillary pressure becomes the dominant stabilizing mechanism. This separation clarifies why classical solidification theory, developed exclusively within the context of Regime A, cannot explain the sustained detached growth observed experimentally in VDS. The quantitative distinction between the two regimes is provided by the stability map shown in Fig. 12 (b). By introducing the Gadkari Detached Stability Criterion, the map explicitly incorporates capillary forces through the Bond and Capillary numbers and defines a stability boundary separating gravity-dominated and capillary-dominated growth. VDS experimental points cluster deep within the capillary-dominated region, demonstrating that surface-tension-driven stabilization overwhelms gravity-induced instabilities when wall contact is eliminated. Dewetted Bridgman growth data occupy an intermediate region, indicating partial capillary stabilization, while microgravity experimental data overlap closely with the VDS regime providing an independent paradigm.

The agreement between VDS and microgravity solidification behavior is particularly significant. Both exhibit diffusion-dominated transport, stable interface morphologies, reduced radial segregation, and improved crystallographic quality. This correspondence demonstrates that gravity reduction is not a prerequisite for achieving microgravity-like solidification conditions. Instead, controlling the force balance at the crystal–melt interface through capillarity provides an alternative and practical route to gravity-resistant growth under 1g conditions.

Overall, the present work resolves a long-standing question in solidification science concerning the persistence of entirely detached growth in the VDS process since its first experimental observations in the mid-1994s. By identifying and quantifying the capillary-dominated stability regime through the Gadkari Detached Stability Criterion, this study establishes a new physical framework that complements, rather than contradicts, classical

gravity-based theories. The results suggest that future crystal growth technologies can exploit capillary control to overcome gravitational limitations, opening new pathways for high-quality crystal growth without reliance on microgravity platforms. **Conceptual separation of solidification regimes:** The conceptual separation of solidification regimes under terrestrial gravity is shown in figures. Regime A corresponds to gravity-influenced wall-contact growth (Fig-12), while Regime B corresponds to capillary-dominated wall-decoupled growth (Fig.13). Figure summarizes the fundamental distinction between the two solidification regimes identified in this work. In Regime A, gravity couples to the melt through wall contact, leading to convection-dominated transport and interface instability governed by classical gravity-based criteria. In Regime B, realized experimentally in the VDS process, wall contact is eliminated and capillary forces dominate the force balance at the solid–liquid interface. This regime lies outside the scope

of conventional solidification theory and requires a separate stability description, provided here by the Gadkari Detached Stability Criterion.

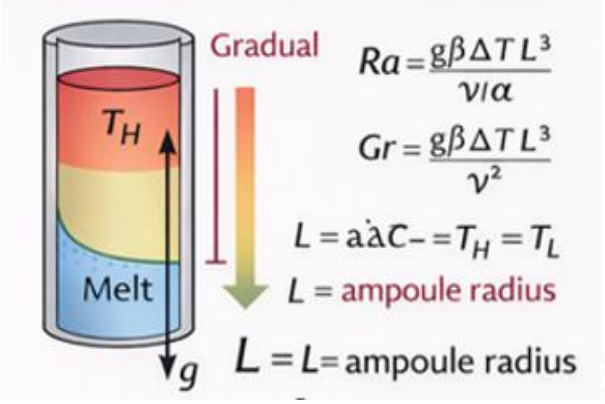

Fig. 12, the classical wall contact growth criteria

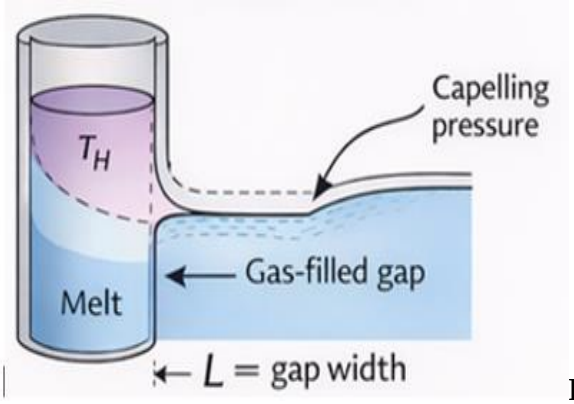

Fig-13 VDS wall-decoupled growth, and the meniscus shape

Stability map based on GDSC: Figure 13 provides a quantitative representation of the two solidification regimes identified schematically in Figures. Data corresponding to conventional wall-contact growth lie in the gravity-dominated region, whereas VDS experimental points cluster deep within the capillary-dominated domain. The stability boundary defined by the *Gadkari Detached Stability Criterion* demonstrates that entirely detached growth under terrestrial gravity arises from capillary stabilization rather than from gravity reduction, explaining the microgravity-equivalent behavior observed in VDS. The stability map in Bond number–Capillary number space illustrating the Gadkari Detached Stability Criterion (Fig.9). The solid curve represents the critical boundary separating gravity-influenced wall-contact growth from capillary-dominated entirely detached growth. Symbols correspond to conventional growth, VDS experiments, dewetted Bridgman growth, and microgravity solidification data.

Two Distinct Solidification Regimes under Terrestrial Gravity: Solidification under terrestrial conditions has historically been interpreted within a single gravity-dominated framework. However, experimental observations in the VDS process demonstrate that two fundamentally different solidification regimes exist, depending on whether the melt is in mechanical contact with the container wall. Significance is the Gadkari Detached Stability Criterion provides the first quantitative framework to explain why entirely detached growth can be sustained under 1g conditions in the VDS process. It formally establishes capillary-dominated solidification as a distinct physical regime, separate from classical gravity-influenced growth, and explains why VDS behaves as a microgravity-equivalent system without reducing gravitational acceleration

Why Conventional Criteria (Ra, Gr, etc.) cannot produce the GDSC Boundary: Classical solidification criteria such as the Rayleigh number (Ra), Grashof number (Gr), Péclet number (Pe), and related stability parameters were developed to describe gravity-driven convection in wall-contact growth systems. These criteria fundamentally differ from the Gadkari Detached Stability Criterion (GDSC) in both assumptions and physical scope, which explains why they cannot produce the stability boundary shown in the Bo–Ca map. Implicit assumption of wall Contact is that the Rayleigh and Grashof numbers are defined as:

$Ra = g\beta\Delta TL^3/\nu\alpha$
$Gr = g\beta\Delta TL^3/\nu^2$

where the characteristic length L is the container radius or melt height. These formulations implicitly assume is mechanical contact between melt and container wall, no-slip boundary condition, direct transmission of gravitational body forces to the melt. Whereas, when wall contact is removed, as in VDS detached growth, these assumptions are violated. The melt is no longer mechanically constrained by the wall, and the characteristic length scale collapses from millimeters to the micrometer-scale gap. Under these conditions, Ra and Gr lose physical meaning as predictors of interface stability. Ra and Gr describe flow onset, not interface detachment, further, Ra and Gr quantify the onset and strength of buoyancy-driven convection in a fluid. They do not address: Meniscus stability, Crystal–melt–gas triple-line force balance, Capillary pressure at curved interfaces. Detached growth is controlled by whether capillary pressure can resist hydrostatic pressur**e**, which is a force-balance problem, not a flow-onset problem. Ra and Gr contain no surface-tension term and therefore cannot describe detachment or wall decoupling. Absence of Capillary Physics: Surface tension (σ) does not appear in Ra or Gr. As a result, Capillary stabilization is entirely absent, Interface curvature effects are ignored, The possibility of capillary-dominated regimes is excluded by construction. In contrast, the GDSC explicitly compares gravity and viscous forces to capillary forces through the Bond and Capillary numbers. This inclusion is essential for describing detached growth.

No Length-Scale Transition in Classical Criteria: The defining feature of detached growth is the change in the relevant transverse length scale:

- Regime-A (wall-contact): L~ ampoule radius (mm–cm)
- Regime-B (entirely detached): L~ gap width (μm)

Classical criteria fix L at the container scale and therefore cannot capture this transition. The GDSC boundary emerges precisely because it is sensitive to this length-scale collapse, which Ra and Gr cannot represent.

Why the GDSC boundary is new: The curved boundary in the Bo–Ca map arises from the condition Bo Ca = constant, which represents a balance between: Gravity-induced pressure, Viscous stress, and Capillary pressure. This balance only becomes relevant after wall contact is removed. Since classical criteria never consider wall-decoupled configurations, they cannot predict or reproduce this boundary.

The results presented in this work demonstrate that entirely detached crystal growth under terrestrial gravity is not an anomalous or transient phenomenon, but the manifestation of a *distinct capillary-dominated solidification regim***e**. The combined experimental observations, schematic representations, and dimensionless analysis establish that the governing physics of the VDS process fundamentally differs from that of conventional wall-contact growth systems.

Classical solidification configuration in which the melt remains in continuous contact with the container wall. Under these conditions, gravitational body forces are transmitted directly to the melt through viscous coupling at the wall, leading to buoyancy-driven convection and three-dimensional transport. Classical gravity-based criteria, including the Rayleigh and Grashof numbers, are therefore applicable and successfully describe flow onset and convection intensity in such systems. However, these criteria implicitly assume wall contact and do not address the stability of the crystal–melt interface when mechanical coupling to the container is removed.

In contrast, the VDS configuration eliminates wall contact over a substantial fraction of the growth length by maintaining a stable gap between the crystal and the ampoule inner wall. This wall decoupling suppresses viscous coupling and prevents direct transmission of gravitational forces to the melt. As a result, the relevant transverse length scale governing stability collapses from the ampoule radius to the micrometer-scale gap width. Experimental evidence confirms that under these conditions, the crystal–melt interface remains stable and entirely detached throughout growth, despite the presence of full terrestrial gravity.

The conceptual separation between these two regimes. Regime A corresponds to gravity-influenced wall-contact growth, where convection dominates transport and interface stability is governed by classical criteria. Regime B corresponds to wall-decoupled growth, where capillary pressure becomes the dominant stabilizing mechanism. This separation clarifies why classical solidification theory, developed exclusively within the context of Regime A, cannot explain the sustained detached growth observed experimentally in VDS.

The quantitative distinction between the two regimes is provided by the stability map. By introducing the Gadkari Detached Stability Criterion, the map explicitly incorporates capillary forces through the Bond and Capillary numbers and defines a stability boundary separating gravity-dominated and capillary-dominated growth. VDS experimental points cluster deep within the capillary-dominated region, demonstrating that surface-tension-driven stabilization overwhelms gravity-induced instabilities when wall contact is eliminated. Dewetted Bridgman growth data occupy an intermediate region, indicating partial capillary stabilization, while microgravity experimental data overlap closely with the VDS regime, providing an independent benchmark.

The agreement between VDS and microgravity solidification behavior is particularly significant. Both exhibit diffusion-dominated transport, stable interface morphologies, reduced radial segregation, and improved crystallographic quality. This correspondence demonstrates that *gravity reduction is not a prerequisite for achieving microgravity-like solidification conditions.* Instead, controlling the force balance at the crystal–melt interface through capillarity provides an alternative and practical route to gravity-resistant growth under 1g conditions.

Overall, the present work resolves a long-standing question in solidification science concerning the persistence of entirely detached growth in the VDS process since its first experimental observations in the mid-1994. By identifying and quantifying the capillary-dominated stability regime through the *Gadkari Detached Stability Criterion*, this study establishes a new physical framework that complements, rather than contradicts, classical gravity-based theories. The results suggest that future crystal growth technologies can exploit capillary control to overcome gravitational limitations, opening new pathways for high-quality crystal growth without reliance on microgravity platforms.

Table 4 The physcical parameters of the InSb,GaSb, doped radicals, ($In_{(1-X)}Ga_XSb$) and $In_{0.5}Ga_{0.5}Sb$ entire detached crystals grown by VDS process

Sr. No	Physical properties	Symbol	InSb	GaSb	InGaSb x=0.5	Quartz	BN

1	Thermal conduct.	k_L (W/m.K	17.7	21.7	17	2.68	54
2	Specific heat	c_{PL} (J/kg K)	350	250	300	1000	2280
3	Viscosity	μ_L (Pa s)	$4x10^{-3}$	$2x10^{-3}$	$3x10^{-3}$		
4	Thermal diffusivity	α_L (m^2/s)	$2.3x10^{-6}$	$1x10^{-5}$	$9.4x10^{-6}$	$10x10^{-6}$	$8.2x10^{-6}$
5	Kinematic viscosity	ν_L (m^2/s)	$3.5x10^{-7}$	$2.7x10^{-7}$	$1.7x10^{-7}$		
6	Latent heat	L (J/Kg)			$3.1x10^5$		
7	Thermal exp. coeff.	β_T (1/K)	4.5×10^{-6}	7.75×10^{-6}	$1x10^{-4}$		
8	Solutal exp. coeff.	β_C (1/K)	5.47×10^{-6}	7.7×10^{-6}	1.0×10^{-4}		
9	Electric conductivity	σ(S/m)	$9.4x10^5$		$1x10^6$		
10	Melting point	T(K)	985	798	978	1610	2973
11	Density (S)	ρ_S (Kg/m^3)	5610	5780	5600	2200	2280
12	Density (L)	ρ_L (Kg/m^3)	6060	6320	6060		
13	Surface tension (L)	γ (N/m)	0.45	0.61	0.50–0.56		
14	Diffusivity (L)	D_l (m^2/s)	$3–5\times10^{-9}$	1×10^{-9}	$1–3\times10^{-9}$		
15	Vapour pressure (P)	P_v (Pa)	$10–10^2$	$10^{-4}–10^0$	$10^{-2}–101$		
16	Partition Coeff.	k	0.13	0.92			

Conclusion

Entirely detached crystal growth in the Vertical Directional Solidification (VDS) process represents a fundamentally distinct solidification regime under terrestrial gravity. Experimental evidence accumulated since the mid-1994s demonstrates that, when wall contact is eliminated, the stability of the crystal–melt interface is governed by capillary pressure rather than by gravity-driven convection. Classical solidification criteria, developed for wall-contact systems, are therefore not applicable to this regime.

By formulating and evaluating the *Gadkari Detached Stability Criterion*, this work provides a quantitative framework that explains the long-standing observation of sustained detached growth in VDS. Numerical analysis shows that VDS operates deeply within a capillary-dominated stability domain, where gravity-induced instabilities are resisted by surface-tension forces. The resulting transport behavior, interface morphology, and crystal quality closely resemble those observed in microgravity experiments.

These findings establish VDS as a practical terrestrial analogue of microgravity solidification and demonstrate that capillary control, rather than gravity reduction, is the key mechanism enabling gravity-resistant crystal growth. The framework presented here resolves a decades-old question (since 1994) in solidification science and opens new pathways for designing crystal growth processes that exploit capillarity to overcome gravitational limitations.

Acknowledgements

The author acknowledges the long-term experimental support and infrastructure that enabled the development of the VDS process and the associated crystal growth studies over multiple decades. The sustained encouragement and technical discussions with colleagues in the fields of crystal growth, solidification physics, and microgravity materials science are gratefully acknowledged. The author expresses sincere gratitude to Prof. B. M. Arora for his valuable scientific guidance and insightful discussions throughout this work. The author also thanks Dr. Shilpa Kalantre for continuous encouragement, Ms. Snehal Gadkari for computational support, and Mrs. Sarojini Gadkari for her unwavering motivation.

Author Contribution: All conceptualization, experimental work, analytical modelling, data interpretation, and manuscript preparation were carried out solely by the author.

Funding: This research received no external funding.

Data Availability: All data supporting the findings of this study are contained within this manuscript.

Competing Interest: The author declares no competing interests.

Conflict of Interest: None declared.

Ethics Approval: Not applicable.
Consent to Participate: Not applicable.

Consent for Publication: Not applicable.

References

1. Akamatsu, S., et al., Solidification patterns under microgravity on the ISS. npj Microgravity **9**, 83 (2023). https://doi.org/10.1038/s41526-023-00326-8
2. Balint, S., Braescu, L., Sylla, L., Epure, S., Duffar, T.: Meniscus shape in dewetted Bridgman growth. Journal of Crystal Growth **310,** 1564–1570 (2008). https://doi.org/10.1016/j.jcrysgro.2007.11.212
3. Balint, S., Epure, S., Duffar, T.: Dewetted Bridgman growth stability, Journal of Engineering Mathematics **75**, 191–208 (2012). https://doi.org/10.1007/s10665-011-9515-z
4. Bergeon, N., Reinhart, G., et al.: Gravity effects during directional solidification. European Physical Journal **44**, 98 (2021). https://doi.org/10.1140/epje/s10189-021-00102-0

5. Bizet, L., Duffar, T.: Stability analysis of dewetted Bridgman growth. Crystal Research and Technology, **39**, 491–500 (2004). https://doi.org/10.1002/crat.200310216
6. Bonn, D., Eggers, J., Indekeu, J., Meunier, J., Rolley, E.: Wetting and spreading, Reviews of Modern Physics. **81**, 739–805 (2009). https://doi.org/10.1103/RevModPhys.81.739
7. Chevalier, N., Dusserre, P., Garandet, J.-P., Duffar, T.: Dewetting application to CdTe crystal growth. Journal of Crystal Growth **261,** 590–594. (2004). https://doi.org/10.1016/j.jcrysgro.2003.10.094
8. Derby, J.J.: Thermal–solutal convection in crystal growth, Journal of Crystal Growth, **360**, 157–164 (2012). https://doi.org/10.1016/j.jcrysgro.2012.08.016
9. Duffar, T., Dusserre, P., Picca, F., Lacroix, S., Giacometti, N.: Bridgman growth without crucible contact using the dewetting phenomenon. Journal of Crystal Growth, **211,** 434–440 (2000). https://doi.org/10.1016/S0022- 0248(99)00775-7
10. Epure, S., Duffar, T., Braescu, L.: Capillary stability of the crystal–crucible gap, Journal of Crystal Growth **312,** 1416–1420 (2010). https://doi.org/10.1016/j.jcrysgro.2009.11.050
11. Gadkari, D.B, Gadkari, D. B., Lal, K. B., Arora, B. M.: Growth of high mobility InSb crystals. (Rapid Communication) J. Crys Growth **175**, 585 (1997)
12. Gadkari, D. B., Lal, K. B., Arora, B. M.: A process for the preparation and orientation growth of single self-seeded crystals of antimonide alloys and/or elementary binary or ternary semiconductors. Indian Patent, (Filed: 139/BOM/1999), Granted No. 192132 (2004)
13. Gadkari, D. B., Arora, B. M.: Detached Solidification Influences the Crystalline Quality of GaSb Crystals Grown by Vertical Directional Solidification Technique on the Earth. Transac. Mater Soc Japan **34**, 571 (2009)
14. Gadkari, D. B.: Advances of the Vertical Directional Solidification Technique for the Growth of High Quality InSb Bulk Crystals. J. Chem. Chem. Eng. **6**, 1 (2012)
15. Gadkari, D. B.: Advances of the Vertical Directional Solidification Technique for the Growth of High-Quality GaSb Bulk Crystal.: J. Chem. Chem. Eng. **6,** 65 (2012)
16. Gadkari Dattatray: Detached Phenomenon and Its Effect on the Thallium Composition into InSb Bulk Crystal Grown by VDS Technique. J. Materi. Sci. Eng. A 2 **(9),** 593 (2012)
17. Gadkari, D. B.: Detached phenomenon: Its influence on the crystal's quality of InSb:Te grown by the VDS technique. AIP Conf. Proc. **1512,** 856 (2013). http://dx.doi.org/10.1063/1.4791308
18. Gadkari, Dattatray: Detached Crystal Growth in VDS Technique: A New Crystal Growth Process. J. Materials Science and Engineering **A 3**(5), 338 (2013)
19. Gadkari Dattatray: Detached phenomenon: Its effect on the crystal quality of Ga (1-x)InxSb bulk crystal grown by the VDS technique Materials Chemistry and Physics 139, 375 (2013) https://doi.org/10.1016/j.matchemphys.2012.09.060
20. Gadkari, D. B.: Detached Growth: Unfolding Four Decades Growth Mystery into Vertical Directional solidification Technique on Earth. In. J. Scien. Resea. Public. 4, 1 (2014)
21. Gadkari Dattatray: Doped InSb Detached Crystals by VDS Technique: Its Substrates for Infrared Devices And Physics Concept. In. J. Engin. Applied Sciences (IJEAS) **2**, 39 (2015)
22. Gadkari1, D., Maske, D., Deshpande, M., Arora B. M.: Detached/Contactless Growths, Reduced Melt Convection and Its Effect on the Device Grade Substrates of Sb-Based Crystals Grown by VDS on Earth. In. J. Innov. Research in Sci. Engin. Techno. 5, **(**2015), doi:10.15680/IJIRSET.2016.0502059 2092

23. Gadkari, D. B.: Detached phenomenon and the fundamental science behind: The novel vertical directional solidification growth of the detached crystals by slow freezing. Int. J. Engin. Rese. Appli. **9**, 1 (2019)
24. Gadkari, D. B.: The homogeneous and entire detached In0.5Ga0.5Sb alloy crystals grown by the slow freezing using novel VDS-process. In. J. Engin. Res. Appli. **10(5)**, 7 (2020)
25. Gadkari, D. B.: Investigation of influence of the indium doping on the properties of the Ga(1-x)InxSb (x=0.10, 0.15, 0.25) crystals: Detached growth by the VDS-process. In. J. Engin. Res. Appli. **10(9)**, 5 2020
26. Gadkari, D. B.: Study of the Ga doped In(1-x)GaxSb (x=0.10, 0.15, 0.25) crystals the compositional, structural, electrical, and the microstructures properties: Growth by the VDS-process. In. J. Engin. Res. Appli. **10(10),** (2020)
27. Gadkari, Dattatray B.: Evaluation of the thermo-diffusion (Soret effect) impact across two phases of the alloys and the crystal-melt interface in In0.5Ga0.5Sb un-seeded crystallization growth by the VDS process. Intern J Engin Res Appli, **11,** 121-132 (2025)
28. Incropera, F.P., Viskanta, R.: Convective heat transfer in crystal growth. Journal of Crystal Growth. 198–199, 129–145 (2000). https://doi.org/10.1016/S0022-0248(98)01041-
29. Kakimoto, K.: Control of convection in bulk crystal growth, Journal of Crystal Growth **275**, 1–10 (2005). https://doi.org/10.1016/j.jcrysgro.2004.10.001
30. Kurz, W., Fisher, D.J.: Fundamentals of solidification revisited. Acta Materialia, **50**, 1857–1874 (2002). https://doi.org/10.1016/S1359-6454(02)00017-3
31. Lan, C.W., Shih, C.J.: Buoyancy-driven convection during directional solidification. Journal of Crystal Growth, **237–239,** 180–186 (2002). https://doi.org/10.1016/S0022-0248(01)02167-6
32. Mazuruk, K., Volz, M.P.: Static stability of menisci in detached growth, Physics of Fluids **25**, 094106 (2013). https://doi.org/10.1063/1.4821849
33. Medjkoune, M., et al.: Benchmark microgravity solidification experiments. Acta Materialia **246**, 120241 (2025). https://doi.org/10.1016/j.actamat.2025.120241
34. Palosz, W., Volz, M.P., Cobb, S.D., Motakef, S., Szofran, F.R.: Detached growth of germanium by directional solidification. Journal of Crystal Growth, 277 (2005) 124–132. https://doi.org/10.1016/j.jcrysgro.2004.12.163
35. Rowlinson, J.S., Widom, B.: Surface tension and capillarity. Reports on Progress in Physics, **69,** 1–44 (2006). https://doi.org/10.1088/0034-4885/69/1/R01
36. Schwabe, D.: Marangoni convection in crystal growth, Advances in Space Research **29,** 1099–1108 (2002). https://doi.org/10.1016/S0273-1177(02)00145-8
37. Stelian, C., Yeckel, A., Derby, J.J.: Crystal reattachment in dewetted growth, Journal of Crystal Growth 311, 2572–2579 (2009). https://doi.org/10.1016/j.jcrysgro.2009.02.01
38. Stelian, C., Volz, M.P., Derby, J.J.: Thermal fields for detached growth, Journal of Crystal Growth **311,** 3337– 3346 (2009). https://doi.org/10.1016/j.jcrysgro.2009.03.04
39. Shevtsova, V., et al.: Thermocapillary instabilities in microgravity, Physics of Fluids **15** 2857–2866. (2003). https://doi.org/10.1063/1.1597471
40. Tourret, D., Karma, A.: Growth competition and interface stability. Acta Materialia **82**, 64–83 (2015). https://doi.org/10.1016/j.actamat.2014.08.048
41. Wang, J., Regel, L.L., Wilcox, W.R.: Detached solidification of InSb on Earth, Journal of Crystal Growth, **260**, 590–599 (2004). https://doi.org/10.1016/j.jcrysgro.2003.09.006

42. Volz, M.P., Mazuruk, K.: Meniscus-controlled crystal growth. Journal of Crystal Growth **321,** 29–35 (2011). https://doi.org/10.1016/j.jcrysgro.2011.02.035
43. Yu, J., et al., InGaSb crystal growth under microgravity, npj Microgravity **5,** 8 (2019). https://doi.org/10.1038/s41526-019-0068-1